Formation of spin-polarons in the ferromagnetic Kondo lattice model away from half-filling

2012 J. Phys.: Condens. Matter 24 335601

(http://iopscience.iop.org/0953-8984/24/33/335601)

IOP PUBLISHING JOURNAL OF PHYSICS: CONDENSED MATTER

J. Phys.: Condens. Matter **24** (2012) 335601 (6pp) doi:10.1088/0953-8984/24/33/335601

Formation of spin-polarons in the ferromagnetic Kondo lattice model away from half-filling

Y Arredondo[1], E Vallejo[2], O Navarro[1] and M Avignon[3]

[1] Instituto de Investigaciones en Materiales, Universidad Nacional Autónoma de México, Apartado Postal 70-360, 04510 México D.F., Mexico
[2] Facultad de Ingeniería Mecánica y Eléctrica, Universidad Autónoma de Coahuila, Carretera Torreón-Matamoros Km. 7.5 Ciudad Universitaria, 27276 Torreón, Coahuila, Mexico
[3] Institut Néel, CNRS and Université Joseph Fourier, Boite Postale 166, 38042 Grenoble, France

E-mail: yesenia@iim.unam.mx

Received 15 February 2012, in final form 1 July 2012
Published 27 July 2012
Online at stacks.iop.org/JPhysCM/24/335601

Abstract

Even though realistic one-dimensional experiments in the field of half-metallic semiconductors are not at hand yet, we are interested in the underlying fundamental physics. In this regard we study a one-dimensional ferromagnetic Kondo lattice model, a model in which a conduction band is coupled ferromagnetically to a background of localized d moments with coupling constant J_H, and investigate the $T = 0$ phase diagram as a function of the antiferromagnetic interaction J between the localized moments and the band-filling n, since it has been observed that doping of the compounds has led to formation of magnetic domains. We explore the spin-polaron formation by looking at the nearest-neighbour correlation functions in the spin and charge regimes for which we use the density matrix renormalization group method, which is a highly efficient method to investigate quasi-one-dimensional strongly correlated systems.

(Some figures may appear in colour only in the online journal)

1. Introduction

Strongly correlated electronic systems are best exemplified in the group of transition-metal and rare-earth compounds. Their half-metallic properties and the possibility of applications in spin-driven devices have triggered intense research in the area of materials science. An example of such materials is the group of manganites with a perovskite structure: the single layered compound $La_xSr_{1+x}MnO_4$ [1], the bilayered compound $La_{2-2x}Sr_{1+2x}Mn_2O_7$ [2] and the cubic compound $La_{1-x}Sr_xMnO_3$ [3]. The magnetotransport of manganites, and in general of ferromagnetic semiconductors, is thoroughly reviewed in [4], where a temperature dependence of the resistivity is described by the magnetoimpurity scattering model there proposed in the framework of the s–d model. Also, a review on some modern approaches on half-metallic ferromagnets is found in [5]. The s–d model, also known as the ferromagnetic Kondo lattice model (KLM), is a generic model to study electrons in a crystal which can be categorized into two subgroups: those electrons which are mobile, the s electrons, not necessarily in the s state, and those electrons which are located into partially occupied d or f shells. Explicitly, the s–f model is studied in relation to the construction of electronic states in the spin-wave region at low temperatures in [6–8]. With transition-metal ions, as is the case of Mn ions in the compounds mentioned above, placed in a crystalline environment of definite symmetry, their d orbitals undergo a break of degeneracy due to the crystal field resulting in three t_{2g} low-energy orbitals and two e_g high-energy state orbitals. Furthermore, lattice effects are also thought to play an important role in the observed insulating behaviour related to a paramagnetic–ferromagnetic transition in the high-temperature regime [9, 10]. Considering that in the case of manganites the d orbitals are not doubly occupied, the t_{2g}

orbitals generate a localized spin background $\vec{S}_i$ with $S = 3/2$ in which electrons move in a linear combination of the two e_g orbitals obeying Hund's rule, which aligns electron spins ferromagnetically when they are on a $\vec{S}_i$ site. Electron mobility is then enhanced if the localized ions are ferromagnetically aligned or restrained in an antiferromagnetic environment. In this regard the ferromagnetic KLM succeeded in explaining the underlying connection between magnetic correlations and spin-dependent transport [11]. In the case of manganites, it is strongly believed that the double-exchange mechanism alone would not suffice to fully understand their magnetic and charge ordering properties, since doping in these materials gives rise to a whole world of magnetic phases from which a consensus regarding the nature of a true ground state in manganites has not yet been reached. Charge order observed in experiments is related to short-ranged antiferromagnetic correlations between the localized spins which break the symmetry of the electron hopping energies [12]. To account for such correlations, antiferromagnetic superexchange interactions are considered such that antiferromagnetic phases, for example in the undoped case of $LaMnO_3$, can be explained. At intermediate band-fillings, however, ferromagnetic interactions, which favour delocalization, and antiferromagnetic interactions between the t_{2g} spins, are competing interactions whose effects have been studied in several intervals. Because of the three t_{2g} levels, models with large S values have been proposed and classical approximations, i.e. in the limit of $J_H \to \infty$, have been studied [13–15]. On-site Coulomb repulsion U is likewise a parameter which has been considered. From results reported in [13], U drives a phase separation for finite superexchange interactions. In [16, 17] a less determinant influence of U on the systems was reported, which is especially the case when classical spins are used.

In this work we investigate numerically the ground-state phase diagram of the one-dimensional Kondo lattice model as a function of the superexchange coupling between nearest-neighbour localized spins as well as a function of the electronic concentration. We use the density matrix renormalization group, which is an efficient method to investigate low-dimensional, many-body systems rendering an accurate description of ground-state properties. We calculate nearest-neighbour spin–spin correlations in order to analyse the magnetic structures generated within different parameter regions.

2. Model and method

We consider the one-dimensional ferromagnetic Kondo lattice model along with superexchange interactions between localized spins with total Hamiltonian

$$\hat{H} = -t \sum_{i,\sigma} c^{\dagger}_{i,\sigma} c_{i+1,\sigma} + \text{h.c.} - J_H \sum_i \vec{S}_i \cdot \vec{\sigma}_i + J \sum_i \vec{S}_i \cdot \vec{S}_{i+1}, \quad (1)$$

where $c^{\dagger}_{i,\sigma}$ ($c_{i,\sigma}$) is the creation (annihilation) operator with spin σ ($=\uparrow, \downarrow$) at site i and $t = 1$ is the nearest-neighbour hopping matrix, which will set our energy scale. $\vec{S}_i$ is the localized spin operator on site i and $\vec{\sigma}_i$ is the electron spin. See figure 1. The Hund and superexchange coupling, $J_H > 0$ and $J \geq 0$ respectively, are given in units of t. The KLM alone gained a great deal of attention due to its applicability in the area of heavy-fermion systems [18]. Furthermore, in the dynamic research field on low-dimensional devices, the one-dimensional version of the KLM is a plausible model to investigate transport properties in structures where a quantum wire is coupled to a ferromagnetic spin chain [19]. The ground-state phase diagram for the KLM is clear only in extreme cases, i.e., at very low carrier concentrations, where for all $|J_H|$ a ferromagnetic phase is identified [20–22], and at half-filling, where for small interactions Kondo singlet formation and Ruderman–Kittel–Kasuya–Yosida (RKKY) interactions occur [23]. In the model of equation (1) ground-state properties as a function of the competing interactions are less well understood. At intermediate values of the charge concentration, as is the case of the doped materials described in section 1, the model has posed a significant challenge in materials science since the magnetic structures arising from key combinations of parameter values do not seem to converge to the same place, apparently making the model under consideration tremendously sensitive to the underlying microscopic structure. Measurement of ground-state properties of the model in equation (1) are carried out using the density matrix renormalization group (DMRG), a well established method which has successfully handled an otherwise exponentially increasing Hilbert space of a low-dimensional, many-body, strongly correlated system [24–29]. Rooted in the numerical renormalization group by Wilson [30], the DMRG method addresses the problem of interacting quantum lattice models by building up iteratively a system from block units representing fermionic or bosonic degrees of freedom. In contrast to the numerical renormalization group by Wilson, which is a method in momentum space, the DMRG method is a real-space method which variationally optimizes the ground state of a given system immersed in a particle bath or reservoir. Treatment of the full Hamiltonian is tackled by performing a systematic decimation of the complete Hilbert space from which a smaller sector of interest is chosen as the subset of the first m most probable states obtained through diagonalization

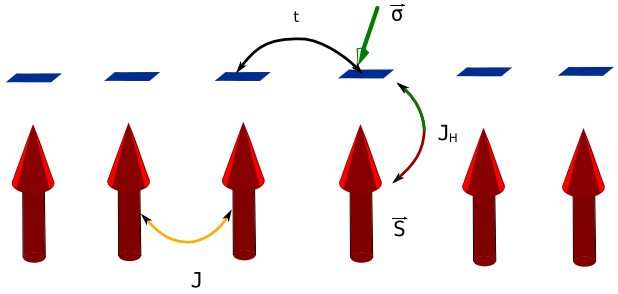

Figure 1. The Kondo lattice model with superexchange interaction J between localized $\vec{S}$ spins. The electrons $\vec{\sigma}$ in the conducting band are coupled ferromagnetically with the localized spins through the Hund coupling constant J_H.

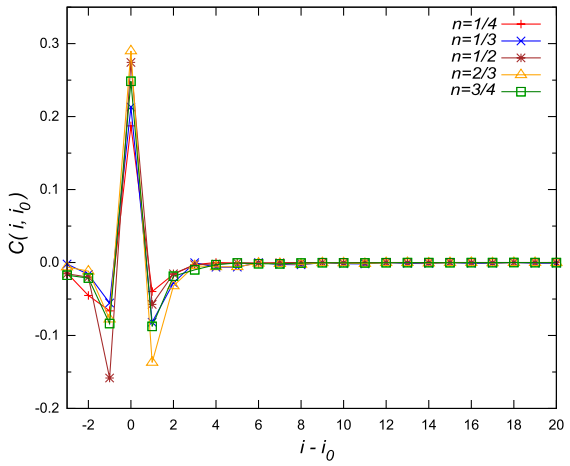

Figure 2. Density–density correlation function $C(i, i_0)$, with $i_0 = 3$, as a function of the band-filling n with $J_H/t = 8.0$ and $J/t = 0.04$.

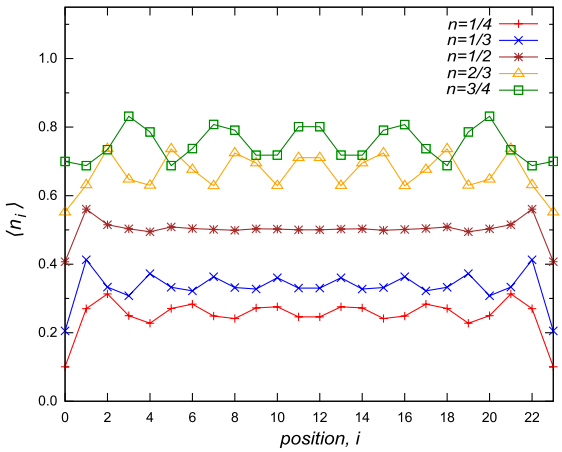

Figure 3. Particle density as a function of the band-filling n with $J_H/t = 8.0$ and $J/t = 0.04$.

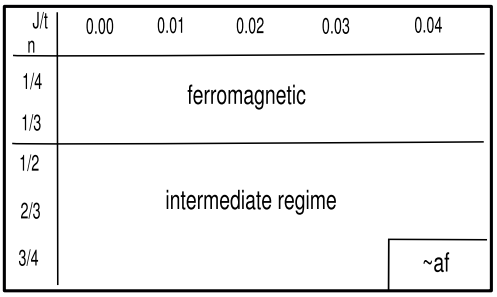

Figure 4. Phase diagram in the spin regime for the model in equation (1) as a function of the band-filling n and the superexchange coupling J. For very low densities a ferromagnetic phase is found, whereas an almost full antiferromagnetic phase, ∼af, is found for higher density and stronger superexchange coupling. In the intermediate regime several magnetic structures are found and described in detail in subsequent figures.

of the density operator of the system. The error generated by the truncation can be examined at every iteration by adding up the weight of the density matrix states discarded. After convergence of the ground-state energy is reached, one can directly measure static expectation values of single operators as well as correlation functions. A great amount of previous work in which the KLM plus superexchange interaction problem is studied also using DMRG is already available [13, 14, 16, 17, 21, 22, 31], and we expect that our findings could confirm some of these results and incline the balance towards a better understanding of the problem. In this work we construct a linear chain of length $L = 24$ sites with one conduction band reminiscent of the e_g level, which will be coupled to a localized spin-1/2 chain with Hund coupling $J_H/t = 8.0$. Localized spins will be left to interact via superexchange coupling interaction with coupling values $J/t = 0$, 0.01, 0.02, 0.03 and 0.04. We present measurements for particle density, density–density and nearest-neighbour spin–spin correlation functions to investigate in some detail the structure of the magnetic ordering away from the half-filled case. In order to achieve better convergence results, the systems modelled in equation (1) are embedded into the DMRG method under open boundary conditions and at least 512 matrix-density states are kept, with a maximum truncation error obtained of approximately 10^{-6}.

3. Results and discussion

To investigate the possible effect of a changing carrier concentration associated with spin-polaron formation in the model of equation (1), we measured the density–density correlation function

$$C(i, i_0) = \langle n_i n_{i_0} \rangle - \langle n_i \rangle \langle n_{i_0} \rangle \qquad (2)$$

as a function of the band-filling. In figure 2 we show our results for $C(i, i_0)$ with superexchange coupling $J/t = 0.04$, although these results hold also for all the other J values in our interval, signalizing that the antiferromagnetic interaction between nearest-neighbour localized spins has no effect whatsoever on the conducting band regardless of the band-filling. From these results, the formation of charge-density waves is ruled out for our systems. On the other hand, if we look at the plain average particle density, $\langle n_i \rangle$, shown in figure 3, one finds finite-size effects such as an oscillating behaviour in the particle distribution. For very low densities the amplitude in the charge-density oscillations is markedly smaller than for densities closer to half-filling, while for a quarter-filling, the particle density distributes rather evenly along the chain.

The ground-state phase diagram in the spin regime was investigated by computing the nearest-neighbour spin–spin correlations on the localized sites $\langle \vec{S}_i \cdot \vec{S}_{i+1} \rangle$ and, as expected, a known magnetic behaviour was found in extreme cases whereas for intermediate electronic concentrations spin arrangements associated to, although not only determined by, charge ordering were observed. Our results on the phase diagram are summarized in figure 4. In [20, 21] the KLM (Hund's model in the last reference) was investigated in the limit of low carrier concentrations and a ferromagnetic ground state was found. Such results correspond to the top-left corner in the phase diagram shown in figure 4, where $J = 0$. We also report a ferromagnetic phase for other values of

the superexchange interaction J in the low-density limit. At the other extreme, at the bottom-right corner, the system with $n = 3/4$ and $J/t = 0.04$ displays an antiferromagnetic ground state up to extremely weakly polarized regions at both ends of the chain. In going from one to the other extreme of the phase diagram, an uneven evolution of the magnetic structures in the ground state is observed. Upon increasing both the carrier concentration and the value of J, spin fluctuations become relevant and generate different ground states, gradually turning the ferromagnetic state into an antiferromagnetic one close to half-filling. In figure 5 we show results for the static spin structure factor S_{zz},

$$S_{zz}(q) = \frac{1}{L}\sum_{i,j} e^{i(r_j - r_i)q}\langle S_i^z S_j^z\rangle. \quad (3)$$

The steadiest magnetic structure was found for the system with a quarter-filled band and $J > 0$, with wavevector $q = \pi/2$. For the $n = 2/3$ case, the spin structure factor does not stabilize as quickly as in the former case. The peaks locate very close to $q = 2\pi/3$, and for $J/t = 0.01$ there is a broader peak at $q = \pi/4$. For a band-filling of $n = 3/4$, there is a steady phase for $0 \leq J/t < 0.03$. For $J/t = 0.04$, the peak departs slightly outwards from the expected value and a broader peak is localized at $q = \pi/4$. In [21] structures found at commensurate wavevectors were labelled as island-like phases, while those found at incommensurate wavevectors were called spiral phases which stands in close relation to the real-space form of the spin–spin correlation function, which we will look at in the coming lines. To gain a deeper insight into the found magnetic structures and to also relate them to the influence of the charge distribution to the different magnetic phases, we plotted for intermediate band-fillings the average particle density along with the local spin–spin correlation function. The phase for $n = 1/2$ is highly uniform, just like the particle density, and extends to all values of J; see figure 6. Such a phase corresponds to an island phase where the localized spins order pairwise in antiferromagnetically aligned polarons as in $\uparrow\uparrow\downarrow\downarrow \cdots \uparrow\uparrow\downarrow\downarrow$. The three phases above described, i.e. the ferromagnetic phase at low densities, the antiferromagnetic at densities close to half-filling, and the island phase at exactly a quarter-filling, have been previously observed in other numerical studies such as [17]. In [13], as well as in [14], their results for the phase diagram, which are alike in their cases, disagree with our results for $1/2 < n < 1$, mainly because they study systems with localized 3/2-spins or classical spins, respectively, which are much greater than in our case. In particular, at quarter-filling they both report ferromagnetic phases where we report an island phase instead. The magnetic phase diagram for the ferromagnetic Kondo model has also been studied in [15]. Their and our results coincide for low densities, finding the ferromagnetic phase. Our incommensurate spin correlations for higher densities agree as well with their results.

With band-fillings greater than $n = 1/2$, a rich variety of magnetic orderings starts appearing as a function of J and can be related to the charge modulation corresponding to these particular concentrations. For $n = 2/3$ three different regions establish along the chain, a left block with pairwise

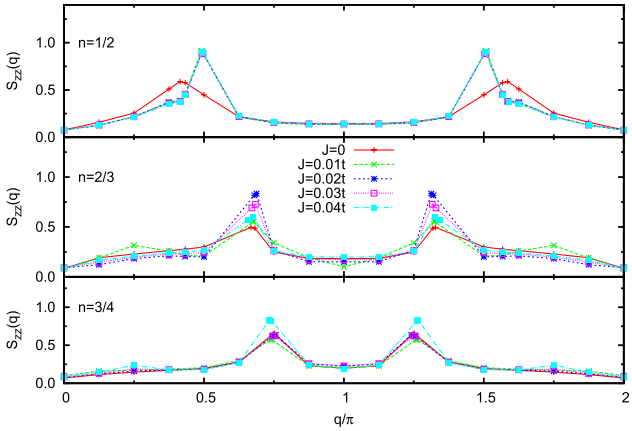

Figure 5. Spin structure factor for different values of the superexchange coupling J and for different band-fillings. The phases found are further detailed in the coming figures and text.

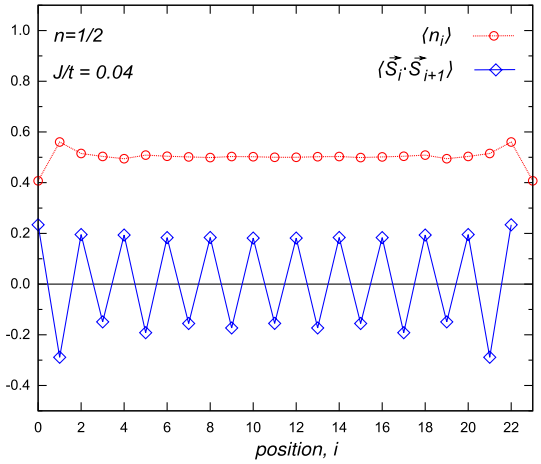

Figure 6. Particle density and nearest-neighbour spin–spin correlation function for $n = 1/2$ and $J = 0.04t$. The magnetic phase found consists of spins ordered pairwise forming polarons ordered antiferromagnetically as in $\uparrow\uparrow\downarrow\downarrow\uparrow\uparrow\downarrow\downarrow$.

polarons aligned in the same direction and separated by a single spin aligned antiferromagnetically, a central block with J-dependent polarization, and a right block also with pairwise polarons all aligned in the same direction, antiparallel to the direction of the polarons in the left block, and separated also by a single spin aligned antiferromagnetically. See figures 7–10. For all values of J the order in both the left and right blocks remains unchanged, whereas an evolution into antiferromagnetic correlations is driven for increasing J only in the central block. For $J/t = 0, 0.01$ there form three spin-polarized zones arranged antiferromagnetically. With $J/t = 0.02, 0.03$ spin flips in the central sites of the block occur leaving pairwise polarons still antiferromagnetically aligned. Once with $J/t = 0.04$, another pair of spin flips takes place leaving the central block with antiparallel arranged single spins. In all cases the peaks of the correlation function are associated with the positions of the minima of $\langle n_i\rangle$, an effect signalizing that it is actually holes around which the magnetic polarons form [13]. For $n = 3/4$ the magnetic phase shown in figure 11 extends over the superexchange coupling

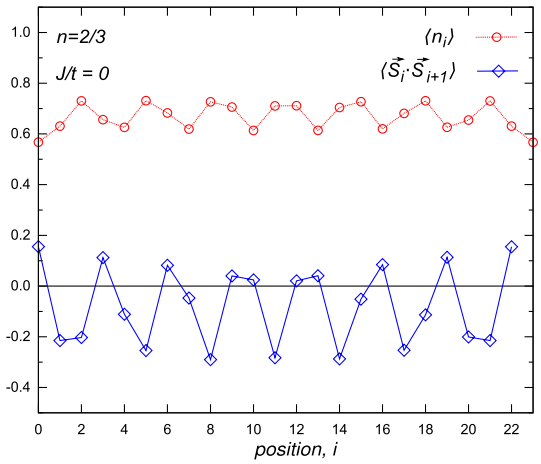

Figure 7. Particle density and nearest-neighbour spin–spin correlation function for $n = 2/3$ and $J/t = 0.0$. Two polaronic structures with three spins each and aligned in opposite directions are found around the middle of the chain.

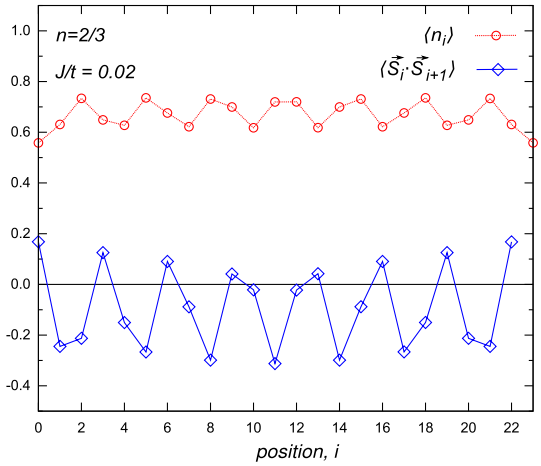

Figure 8. Particle density and nearest-neighbour spin–spin correlation function for $n = 2/3$ and $J/t = 0.02$. The influence of the superexchange coupling causes spin flips around the middle of the chain, generating structures of two-spin polarons.

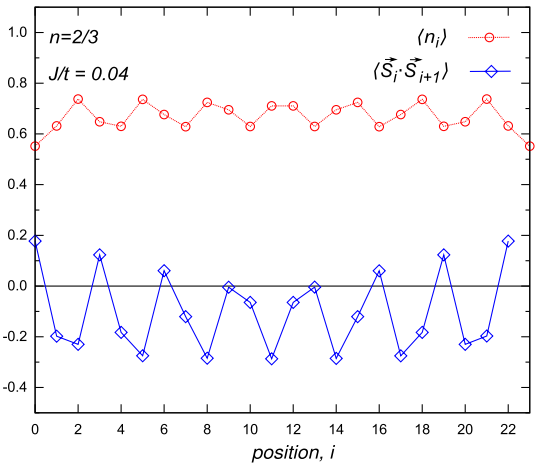

Figure 9. Particle density and nearest-neighbour spin–spin correlation function for $n = 2/3$ and $J = 0.04t$. The central polaronic structure is destroyed and an antiferromagnetic one forms.

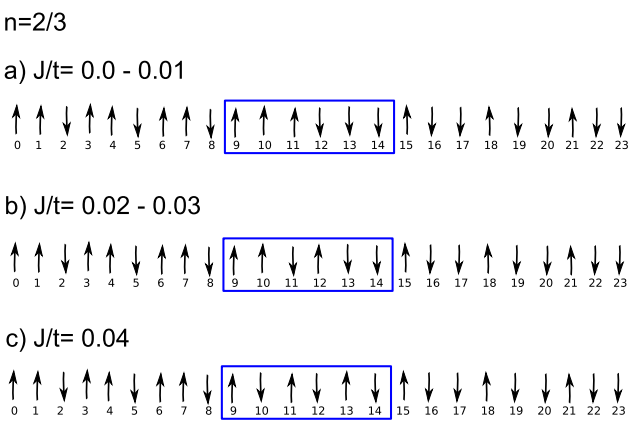

Figure 10. Summary of spin-polarized regions for $n = 2/3$ as a function of the superexchange coupling J, which causes a central polarization to evolve into an antiferromagnetic ordered region.

from $J/t = 0$ up to 0.03. It consists of an arrangement of two-spin polarons antiferromagnetically ordered and intercalated with $\downarrow\uparrow$ and $\uparrow\downarrow$ spin pairs. With $J/t = 0.04$ the spins align antiferromagnetically along the chain and only two-spin polarons barely survive at both ends of the system. See figures 12 and 13. Note that, in this case, the valleys in the charge distribution do not pin a polaron anymore; however, they are still related to the peaks in the spin–spin correlation function. It is interesting to observe that, although the phase shows antiferromagnetic correlations up to the endings of the chain, such results are not reflected in the spin structure factor. The evolution of this phase is rather drastic compared to the $n = 2/3$ case.

4. Summary and conclusions

In this work we investigated magnetic ordering in one-dimensional systems where a conduction band is coupled to a spin background and for which the ground-state phase diagram is not fully understood. Some key cases such as ferromagnetic, island and antiferromagnetic phases, as reported in [16, 17, 21], were found. Still, the carrier concentration interval $1/2 < n < 1$ seems to offer a very sensitive behaviour. It seems that the relation between charge distribution and the formation of magnetic regimes holds only in one direction; i.e., an oscillating charge distribution due to particle densities away from half-filling in finite systems does not necessarily imply the formation of distinct polarized regions, as was the case for $n = 1/4, 1/3$. However, polarons can be associated with holes, which seemed to pin down some of the magnetic structures. It is the superexchange coupling between the localized spins which drives and details the ordering of the spins in the end. Furthermore, [32] reported on the contributions of the diagonal part S^zS^z or transverse scattering associated with the S^+ and S^- operators in experiments of quasielastic scattering in $La_{0.67}Ca_{0.33}MnO_3$. Our findings show that precisely for the $n = 2/3$ case

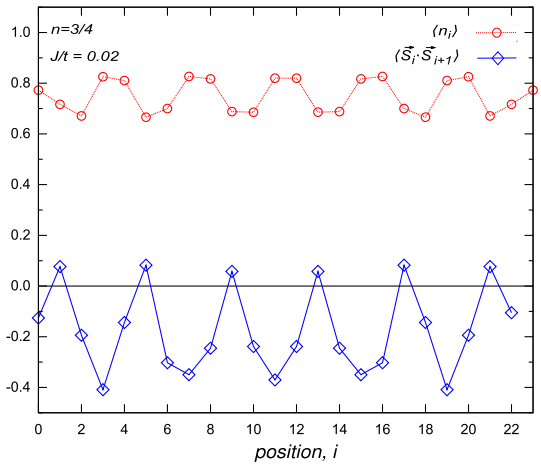

Figure 11. Particle density and nearest-neighbour spin–spin correlation function for $n = 3/4$ and $J/t = 0.02$. The same behaviour is found for $J = 0$ up to $J = 0.03t$ with two-spin polarons found alternating antiferromagnetically.

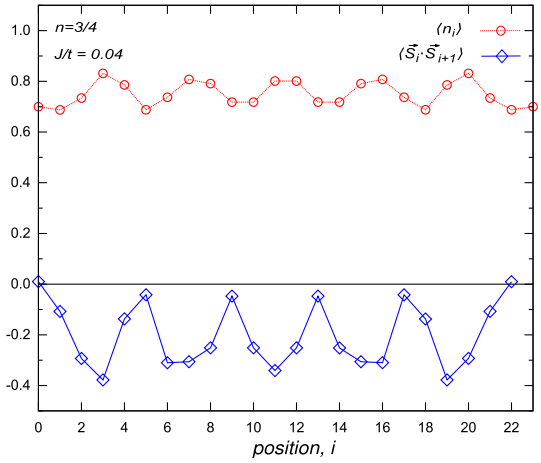

Figure 12. Particle density and nearest-neighbour spin–spin correlation function for $n = 3/4$ and $J/t = 0.04$. Up to two polarons at the edge of the chain, the system behaves antiferromagnetically.

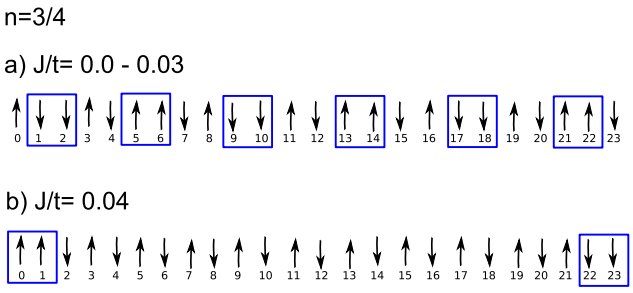

Figure 13. Summary of spin-polarized regions for $n = 3/4$ as a function of the superexchange coupling J, which causes an alternating polarization to evolve into an antiferromagnetically ordered region.

(corresponding to a doping of $x = 1/3$) both diagonal and off-diagonal spin contributions are important, this not being the case for other concentrations.

Acknowledgments

This work has been partially supported by grant 131589 from CONACYT and by PAPIIT-IN108710 from UNAM. YA would like also to acknowledge full financial support by grants from DGAPA-UNAM and CONACYT.

References

[1] Merz M, Roth G, Reutler P, Büchner B, Arena D, Dvorak J, Idzerda Y U, Tokumitsu S and Schuppler S 2006 *Phys. Rev.* B **74** 184414
[2] Koizumi A, Miyaki S, Kakutani Y, Koizumi H, Hiraoka N, Makoshi K, Sakai N, Hirota K and Murakami Y 2001 *Phys. Rev. Lett.* **86** 5589
[3] Furukawa N 2002 Thermodynamics of the double exchange systems *Physics of Manganites* ed T A Kaplan and S D Mahanti (New York: Kluwer Academic) pp 1–38
[4] Nagaev E L 2001 *Phys. Rep.* **346** 387
[5] Katsnelson M I, Irkhin V Yu, Chioncel L, Lichtenstein A I and de Groot R A 2008 *Rev. Mod. Phys.* **80** 315
[6] Auslender M I, Katsnelson M I and Irkhin V Yu 1983 *Physica* B+C **119** 309
[7] Auslender M I, Irkhin V Yu and Katsnelson M I 1984 *J. Phys. C: Solid State Phys.* **17** 669
[8] Auslender M I and Irkhin V Yu 1985 *J. Phys. C: Solid State Phys.* **18** 3533
[9] Millis A J 1998 *Nature* **392** 147
[10] Schmidt R, Eerenstein W and Midgley P A 2009 *Phys. Rev.* B **79** 214107
[11] Kubo K and Ohata N 1972 *J. Phys. Soc. Japan* **33** 21
[12] Solovyev I V 2003 *Phys. Rev. Lett.* **91** 177201
[13] Neuber D R, Daghofer M, Evertz H G, von der Linden W and Noack R M 2006 *Phys. Rev.* B **73** 014401
[14] Vallejo E, López-Urías F, Navarro O and Avignon M 2009 *Solid State Commun.* **149** 126
[15] Dagotto E, Yunoki S, Malvezzi A L, Moreo A, Hu J, Capponi S, Poilblanc D and Furukawa N 1998 *Phys. Rev.* B **58** 6414
[16] García D J, Hallberg K, Batista C D, Avignon M and Alascio B 2000 *Phys. Rev. Lett.* **85** 3720–3
[17] García D J, Hallberg K, Batista C D, Capponi S, Poilblanc D, Avignon M and Alascio B 2002 *Phys. Rev.* B **65** 134444
[18] Hewson A C 1997 *The Kondo Problem to Heavy Fermions* (Cambridge: Cambridge University Press)
[19] Reininghaus F, Korb T and Schoeller H 2006 *Phys. Rev. Lett.* **97** 026803
[20] Sigrist M, Ueda K and Tsunetsugu H 1992 *Phys. Rev.* B **46** 175
[21] García D J, Hallberg K, Alascio B and Avignon M 2004 *Phys. Rev. Lett.* **93** 177204
[22] Smerat S, Schollwöck U, McCulloch I P and Schoeller H 2009 *Phys. Rev.* B **79** 235107
[23] Clare C Yu and Steven R W 1993 *Phys. Rev. Lett.* **71** 3866
[24] White S R 1993 *Phys. Rev.* B **48** 10345
[25] Noack R M and White S R 1999 The density matrix renormalization group *Density Matrix Renormalization: A New Numerical Method in Physics* (*Lecture Notes in Physics* vol 528) ed I Peschel, X Wang, M Kaulke and K Hallberg (Berlin: Springer) pp 27–66
[26] Schollwöck U 2005 *Rev. Mod. Phys.* **77** 259
[27] Hallberg K 2006 *Adv. Phys.* **55** 477
[28] Arredondo Y and Monien H 2008 *Phys. Rev.* B **78** 115425
[29] Arredondo Y and Navarro O 2010 *Solid State Commun.* **150** 1313
[30] Wilson K 1975 *Rev. Mod. Phys.* **47** 773
[31] McCulloch I P, Juozapavicius A and Rosengren A 2001 *Phil. Mag. Lett.* **81** 869
[32] Lynn J W, Erwin R W, Borchers J A, Huang Q, Santoro A, Peng J-L and Li Z Y 1996 *Phys. Rev. Lett.* **76** 4046–9